Vol. 652: 49–62, 2020
https://doi.org/10.3354/meps13474

MARINE ECOLOGY PROGRESS SERIES
Mar Ecol Prog Ser

Published October 15

Effect of temperature and feeding on carbon budgets and O_2 dynamics in *Pocillopora damicornis*

Niclas Heidelberg Lyndby[1,5,*], Jacob Boiesen Holm[1], Daniel Wangpraseurt[1,2,3], Renaud Grover[4], Cécile Rottier[4], Michael Kühl[1], Christine Ferrier-Pagès[4]

[1]Marine Biological Section, Department of Biology, University of Copenhagen, Strandpromenaden 5, 3000 Helsingør, Denmark
[2]Marine Biology Research Division, Scripps Institution of Oceanography, 9500 Gilman Drive, La Jolla, California 92093, USA
[3]Bioinspired Photonics Group, Department of Chemistry, University of Cambridge, CB2 1EW Cambridge, UK
[4]Centre Scientifique de Monaco, Coral ecophysiology team, 8 quai Antoine 1er, 98000 Monaco

[5]*Present address:* Laboratory for Biological Geochemistry, School of Architecture, Civil and Environmental Engineering, Ecole Polytechnique Fédérale de Lausanne, 1015 Lausanne, Switzerland

ABSTRACT: Studying carbon dynamics in the coral holobiont provides essential knowledge of nutritional strategies and is thus central to understanding coral ecophysiology. In this study, we assessed the carbon budget in *Pocillopora damicornis* (using $H^{13}CO_3$) as a function of feeding status and temperature stress. We also compared dissolved oxygen (O_2) fluxes measured at the colony scale and at the polyp scale. At both scales, O_2 production rates were enhanced for fed vs. unfed corals, and unfed corals exhibited higher bleaching and reduced photosynthetic activity at high temperature. Unfed corals exclusively respired autotrophically acquired carbon, while fed corals mostly respired heterotrophically acquired carbon. As a consequence, fed corals excreted on average >5 times more organic carbon than unfed corals. Photosynthate translocation was higher under thermal stress, but most of the carbon was lost via respiration and/or mucus release (42–46% and 57–75% of the fixed carbon for unfed and fed corals, respectively). Such high loss of translocated carbon, coupled to low assimilation rates in the coral tissue and symbionts, suggests that *P. damicornis* was nitrogen and/or phosphorus limited. Heterotrophy might thus cover a larger portion of the nutritional demand for *P. damicornis* than previously assumed. Our results suggest that active feeding plays a fundamental role in metabolic dynamics and bleaching susceptibility of corals.

KEY WORDS: Coral bleaching · Photobiology · ^{13}C · Carbon dynamics · Carbon budget · Heterotrophy · Autotrophy

1. INTRODUCTION

Coral reefs in tropical and subtropical regions are primarily formed by calcifying (scleractinian) corals that are fueled by an endosymbiotic relationship between the cnidarian hosts and their photosynthesizing symbionts from the dinoflagellate family Symbiodiniaceae (LaJeunesse et al. 2018). This mutualistic relationship enables corals to thrive in oligotrophic waters by relying on nutrient transfer between the animal host and its photosynthesizing symbionts (Muscatine & Cernichiari 1969, Muscatine et al. 1981, Tremblay et al. 2012).

It is generally accepted that in corals, symbiont photosynthesis can cover up to 95% of the daily energy demand of the animal host (Davies 1984, Muscatine et al. 1984, Edmunds & Davies 1986), especially in shallow waters where photosynthetically active radiation (PAR) is not limiting. However, corals that inhabit deeper and/or turbid waters are far more dependent on active feeding, as photosynthesis becomes light limited (Falkowski et al. 1984, Palardy et

*Corresponding author: niclas.lyndby@epfl.ch

al. 2008). Corals of the photic zone utilize heterotrophy for supplementary carbon and nutrient acquisition, even in high light environments. This implies an advantageous effect from active feeding (Wellington 1982, Sebens et al. 1996, Houlbrèque et al. 2004), where corals rely on heterotrophy for acquiring nitrogen, phosphorus, and other essential nutrients that cannot be acquired otherwise (Houlbrèque & Ferrier-Pagès 2009).

Heterotrophy becomes particularly important during bleaching events, as corals rely on symbionts to sustain their daily metabolic energy demand. The loss of symbionts induces coral starvation and in extreme events leads to death of corals and regime shifts of entire reef ecosystems (Brown 1997, Hoegh-Guldberg et al. 2017, Hughes et al. 2017). In addition, coral bleaching can lead to an 'optical feedback loop,' where symbiont loss promotes increased tissue light penetration, skeletal backscattering, and enhanced light absorption by the remaining dinoflagellates (Enriquez et al. 2005, Wangpraseurt et al. 2017). This causes additional photodamage and production of reactive oxygen species (ROS), which accelerate the bleaching process (Lesser 1996, Weis 2008, Gardner et al. 2017). In such conditions, heterotrophy increases energy stores of macromolecules such as lipids (Hughes & Grottoli 2013, Towle et al. 2015), sustaining coral host metabolism and the repopulation of dinoflagellates during advantageous environmental conditions (Grottoli et al. 2006, Rodrigues & Grottoli 2007, Hughes et al. 2010). During bleaching, the relative input of carbon from heterotrophy compared to autotrophy can be up to 100% in certain coral species (Grottoli et al. 2006, Courtial et al. 2017). This suggests species-specific adaptions among corals to utilize active feeding as a primary nutrient source under stressed conditions. Many other factors interact with heterotrophy to mitigate coral bleaching. For example, corals can increase transfer of photosynthates by the remaining symbionts (Tremblay et al. 2016) or decrease their metabolism (as assessed by the decrease in respiration rates and carbon release) during stress (Storey & Storey 1990, Jacobson et al. 2016).

However, the energetic demand of corals during thermal stress is poorly understood, and key physiological parameters such as respiration and gross photosynthesis are often determined with insufficient spatial and temporal resolution to obtain accurate values (Kühl et al. 1996, Schrameyer et al. 2014). Indeed, daytime respiration assessed with dark incubations by respirometry on a colony/fragment scale (macroscale) is often underestimated, because O_2 produced by symbiont photosynthesis is used immediately for symbiont and coral respiration, leading to an overall higher respiration during photoperiods (Kühl et al. 1995). This intimate association between autotrophic and heterotrophic processes makes the quantitative and spatial separation of respiration and photosynthesis difficult (Kühl et al. 1995, 1996). The use of fast-responding O_2 microsensors allows for assessing true gross photosynthesis and light respiration rates (Revsbech & Jørgensen 1983, Schrameyer et al. 2014). Thus, the first aim of our study was to compare O_2 dynamics obtained by respirometry at the colony scale to measurements performed with O_2 microsensors at the polyp scale. The second critical step for the assessment of the amount of energy received by the coral host through auto- and heterotrophic processes is to quantify photosynthate production and transfer by the symbionts. Translocation rates can be assessed by calculating a carbon budget for corals through the use of ^{13}C-isotope tracer experiments and determination of O_2 fluxes (Tremblay et al. 2012). The combination of the 2 techniques allows quantification of (1) autotrophic carbon fixation rates, (2) the fraction of carbon stored in symbionts and host tissue, and (3) the fraction of carbon lost through respiration and mucus release. The assessment of symbiont gross photosynthesis rates and photosynthate translocation to the coral host provides insight into the role of heterotrophy on coral resistance to thermal stress.

2. MATERIALS AND METHODS

2.1. Corals

Nubbins of *Pocillopora* sp. (presumed *P. damicornis*) cultured at the Centre Scientifique de Monaco (CSM), were prepared by cutting 8 mother colonies into 128 fragments of 2–3 cm in length (16 fragments per colony) that were hung from nylon threads in several glass aquaria. Two months prior to the bleaching experiment, 16 fragments per colony were divided into 8 fed and 8 unfed nubbins, which were again separated into 4 fed and 4 unfed tanks (2 nubbins per mother colony and per tank = 16 fragments per tank). All nubbins were kept under white light (250 W metal halide lamps) for 12 h d^{-1}, at a downwelling photon irradiance (400–700 nm) of 250 ± 20 µmol photons m^{-2} s^{-1}, as measured with a calibrated spectroradiometer (MSC-15, GigaHertz-Optik). As aquaria were made of transparent glass and were placed on a highly reflective white bench, light reaching the nubbins was

similar between the upper and lower side of the nubbins. Fed corals were fed 4 times per week with ~4000 *Artemia* nauplii per coral fragment per day with the tank flow turned off until aquaria were visibly empty of prey. Unfed corals were heterotrophically starved throughout the study, including the 2 mo prior to measurements. The symbiont clade hosted by all colonies of *P. damicornis* used in this study was identified as the genus *Cladocopium* (previously clade C; LaJeunesse et al. 2018) using chloroplastic ribosomal DNA sequences (Godinot et al. 2013).

At the beginning of the study, the water temperature was set to 25°C for all tanks. One tank per feeding treatment was then kept as a control, while 3 other tanks were used for exposing corals to thermal stress by gradually ramping water temperature up to 30°C over a period of 5 d, at a rate of 1°C d^{-1}. Thermally stressed corals were kept at 30°C for an additional 3 d before starting measurements. Coral measurements after 3 d of 30°C thermal stress are denoted as time point 1 (T_1). After an additional 5 d of thermal stress, measurements were conducted again at time point 2 (T_2). Measurements on control corals were done during the time period between T_1 and T_2, and are denoted time point 0 (T_0). No measurements were performed on unfed corals after 8 d of stress (T_2) due to significant bleaching, which impaired measurements. For an overview of the experimental timeline, see Fig. A1 in the Appendix.

2.2. Experimental setup and approach

Microsensor measurements were performed on corals placed in a black acrylic flow chamber, which was supplied with seawater (25°C, salinity 35‰) from a heated water reservoir (10 l) at a flow rate of ~0.25 cm s^{-1}. A motorized micromanipulator (MU-1, PyroScience) was attached to a heavy duty stand to facilitate positioning of microsensors on fragments at a 45° angle relative to the vertically incident light. A digital microscope (Dino-Lite Edge AM7515MZTL, AnMo Electronics) was used for observation, while carefully positioning the microsensor tip onto the coral tissue surface. Corals were illuminated from above with white light provided by a tungsten halogen lamp with an internal heat filter (KL-2500 LCD, Schott) and fitted with a fiber-optic light guide and a collimating lens. A calibrated spectroradiometer (MSC-15, GigaHertz-Optik) was used to quantify the absolute downwelling photon irradiance (PAR, 400–700 nm) at different lamp settings (80, 167, 250, 480, 970, and 2400 µmol photons m^{-2} s^{-1}), and to record downwelling irradiance spectra in units of W m^{-2} nm^{-1}. The irradiance was adjusted without changing spectral composition by adjusting a metal disk with varying perforation between the halogen light bulb and the fiber-optic light guide in the lamp light path. Setups were covered with black cloth during measurements to avoid stray light. For each coral replicate used in this study, microsensor measurements were done on 3 randomly chosen polyps located on the branch tips. Further details of the experimental setup are described by Lyndby et al. (2019).

2.3. Microsensor measurements

Gross photosynthesis was measured with Clark-type O_2 microelectrodes with a tip diameter of ~25 µm, a low stirring sensitivity (<5%), and a fast response time (<0.5 s; OX-25 fast, Unisense). The microelectrodes were connected to a pA meter (Unisense) and were linearly calibrated from readings in 100% air-saturated seawater and anoxic water (by addition of Na_2SO_3) at experimental temperature and salinity. The corresponding O_2 concentration (µmol l^{-1}) in seawater at 100% air saturation was taken from gas tables for the O_2 solubility in air-saturated water as a function of temperature and salinity (provided by Unisense). Data were recorded on a strip-chart recorder (BD25, Kipp & Zonen) connected to the pA meter. Gross photosynthesis was estimated using the light–dark shift method as described in detail by Revsbech & Jørgensen (1983), where the measurements performed at the coral tissue surface were regarded as representative of the entire tissue volume of *P. damicornis* given that the tissue thickness in most places was ~100–200 µm, which approximates the spatial resolution of the light–dark shift method during the 2–3 s period of darkening. The areal rate of gross photosynthesis was estimated by multiplying the measured volume-specific gross photosynthesis at the tissue surface (in nmol O_2 cm^{-3} s^{-1}) by the local tissue thickness (in cm). The local tissue thickness was estimated from the difference in depth position of scalar irradiance measurements done at the water–tissue and tissue–skeleton interface, respectively (see Lyndby et al. 2019).

For measurements of holobiont dark respiration (R), coral fragments were dark acclimated for 15 min before measuring O_2 concentration profiles across the diffusive boundary layer (DBL) between the mixed overlying water and the coral tissue surface. Measurements started at the tissue surface (depth = 0 µm), and the microsensor tip was moved upwards

in steps of 50 µm (10 s rest time per measuring position) until reaching the ambient water with a constant O_2 concentration (of 100% air saturation).

Subsequently, net photosynthesis vs. irradiance curves were measured under 7 increasing levels of incident photon scalar irradiance (see Section 2.2). Each coral fragment was incubated for 10 min at each irradiance level, ensuring steady-state conditions. A total of 4 replicate fragments were measured per treatment and time point using 3 randomly selected polyps, i.e. a total of 12 measurements per treatment and time point.

Local net photosynthesis (P_n) and R rates were determined as the net O_2 flux, J (nmol O_2 cm^{-2} s^{-1}), as calculated from the measured steady-state O_2 profiles using Fick's first law of diffusion:

$$J = D_0 \frac{\delta C}{\delta z} \quad (1)$$

where D_0 is the molecular diffusion coefficient of O_2 in seawater at experimental salinity (in per mille) and temperature ($D_0 = 2.23 \times 10^{-5}$ cm^2 s^{-1} at 25°C and 35‰, and $D_0 = 2.55 \times 10^{-5}$ cm^2 s^{-1} at 30°C and 35‰), $\delta C/\delta z$ is the slope of the linear part of the O_2 concentration gradient in the DBL, defined by the change in O_2 concentration (δC) over a specific depth interval (δz).

2.4. Gas exchange measurements

Additional respiration and photosynthesis measurements were made by measuring the net O_2 gas exchange of coral fragments (Hoogenboom et al. 2010) under photon scalar irradiance levels of 0, 50, 100, 200, and 400 µmol photons m^{-2} s^{-1}. For this, coral fragments (3–5 for each treatment) were positioned in individual small incubation chambers (50 ml), and the fragments were illuminated from the side with a 250 W metal halide lamp. To ensure even illumination of the entire coral fragment, aluminum foil was placed behind the incubation chamber, reflecting the incident beam and illuminating the otherwise shaded areas of the coral fragment. The photon scalar irradiance in the incubation chamber was measured for defined lamp settings using a spherical mini quantum sensor (sphere diameter of 3.7 mm, US-SQS/L, Walz) attached to a light meter (LI-190, Li-Cor).

The temperature in the experimental chambers was kept at 25°C for control and at 30°C for heat-treated fragments, and the chambers were constantly stirred with a magnet. The O_2 concentration was logged over time with an O_2 optode, connected to a computer with Oxy-4 software (4-channel fiber-optic O_2 meter; PreSens). O_2 optodes were linearly calibrated from measurements in air-saturated water (bubbled with air) and anoxic water (flushed with N_2) according to the manufacturer's recommendations.

Holobiont respiration, R, was determined as the O_2 depletion rate after 15 min dark adaptation, and post-illumination respiration as the initial post-illumination O_2 depletion rate after each experimental irradiance level. P_n was determined as the O_2 concentration increase rate after 15 min illumination at the given photon irradiance similar to post-illumination respiration measurements. The O_2 depletion and production curves were fitted with linear regression and rates of respiration and net-photosynthesis were calculated as:

$$P_n \text{ and } R = \left\{\left[\left(\frac{\left(\frac{\Delta\%C}{\Delta t} \bullet sol_{O_2}\right)}{100\%}\right) \bullet \frac{P_{chamber}}{P_{atmospheric}}\right] \bullet 60 \text{ min}\right\} \bullet \frac{V_{chamber}}{1000 \text{ ml}} \quad (2)$$

where $\Delta\%C/\Delta t$ is the change in $\%O_2$ over time (% min^{-1}), sol_{O_2} is the O_2 solubility (µmol l^{-1}) for the given temperature and salinity (sol_{O_2} = 211.3 µmol l^{-1} at 25°C and 35‰, and sol_{O_2} = 194.6 µmol l^{-1} at 30°C and 35‰), $P_{chamber}$ / $P_{atmospheric}$ is the relative difference in partial pressure (hPa) between atmospheric air and the water mass in the incubation chamber, $V_{chamber}$ is the volume of the chamber corrected from the volume of the coral nubbin (ml), and P_n and R are rates of net O_2 production and O_2 consumption per coral area (in µmol O_2 cm^{-2} h^{-1}), respectively. Rates of gross photosynthesis (P_g) were then estimated by adding R to P_n. All rates were normalized to coral surface area, which was assessed with the wax dipping technique according to Veal et al. (2010).

Furthermore, O_2 gas exchange was measured on freshly isolated symbionts from 3 previously measured fragments. The symbionts were extracted from 3 fragments per treatment and time point by first removing the coral tissue using an airbrush with 35 ml filtered seawater (FSW; 0.45 µm). The removed tissue was homogenized with a Potter tissue grinder and transferred to a 50 ml Falcon® tube that was centrifuged at 850 × g (10 min). After removal of the supernatant, the remaining symbiont pellet was resuspended in FSW (0.45 µm).

The symbiont density was quantified in a 100 µl sub-sample using a Z1 Coulter Particle Counter (Beckman Coulter). The surface area of the nubbin from which symbionts were extracted was also determined. The O_2 fluxes were estimated using similar techniques as whole fragment measurements described previously, and were converted to carbon units according to Anthony & Fabricius (2000):

$$P_c = P_g \bullet \left(\frac{12}{Q_{phot}} \right) \quad (3)$$

$$R_C = R \bullet (12 \bullet Q_{resp}) \quad (4)$$

where P_c is the total amount of inorganic C fixed through photosynthesis, P_g is the gross O_2 production calculated from P_n and R in µmol O_2 cm^{-2} h^{-1}; 12 is the mass of a carbon atom, Q_{phot} is the photosynthetic quotient, here assumed to be 1.1 mol O_2:mol C (Muscatine et al. 1981), R_C is the rate of consumed inorganic C (µg C m^{-2} h^{-1}) by respiration R, and Q_{resp} is the respiratory quotient, assumed to be equal to 0.8 mol C:mol O_2 (Muscatine et al. 1981).

2.5. $H^{13}CO_3$ tracer incubations

Corals used for stable isotope incubations with $H^{13}CO_3$ were mounted in beakers incubated with FSW (controls) or ^{13}C-enriched FSW (treatments) for pulse labeling periods of 4 h (Tremblay et al. 2012). The treated fragments were exposed to a solution of 0.6 mM $NaH^{13}CO_3$ (98% ^{13}C; no. 372382, Sigma-Aldrich), mixed with 200 ml FSW (Tremblay et al. 2012). The beakers were left open and the solutions were constantly stirred by a magnet bar.

The beakers with fragments of *P. damicornis* (3–5 for each treatment, 1 fragment per beaker) were kept in a temperature-regulated water bath at a constant temperature of 25°C (control) or 30°C (heat-stress) under a constant incident photon irradiance (400–700 nm) of 200 µmol photons m^{-2} s^{-1}. During these incubations, O_2 production and consumption were not recorded, but the rates of carbon fixation and respiration were derived from the above mentioned O_2 gas exchange measurements on intact corals at 200 µmol photons m^{-2} s^{-1}. For quantification of ^{13}C enrichment in coral fragments, the tissue was detached from the skeleton by an air brush with 10 ml FSW. The tissue slurry was homogenized with a Potter tissue grinder, and the animal and symbiont fractions were then separated several times by centrifugation (1328 × *g* for 5 min). Tissue and symbionts were separated, then frozen in liquid N_2 and freeze-dried for later analysis. The ^{13}C enrichment and carbon content in the animal tissue and symbionts were quantified with a mass spectrometer (Delta Plus, Thermo Fisher Scientific) coupled via a type III interface with a C/N analyzer (Flash EA, Thermo Fisher Scientific), and compared with $^{13}C/^{12}C$ in the control fragments. The carbon budget was then calculated using the equations described by Tremblay et al. (2012). See Fig. 1 for a schematic overview of the carbon budget and its pathways.

2.6. Statistical analysis

All data included in ANOVA tests were verified for normal distributions using Shapiro-Wilk tests with a significance level of $\alpha = 0.05$, along with the Brown-Forsythe test to ensure data was of equal variance. All statistical analyses were performed in OriginPro 2020b (version 9.7.5.184 [academic], OriginLab).

We used 2-way ANOVAs with a significance level of $\alpha = 0.05$ to test for effects of heat stress and feeding status at T_0 and T_1 (after 8 d of heat stress). Additionally, 1-way ANOVAs were performed on data from fed corals to include comparisons with fed corals maintained for 13 d under heat stress (T_2 data). Tukey post hoc analyses with a significance level of $\alpha = 0.05$ were performed on all relevant tests where more than 2 groups were involved.

For data including several light intensities (area- and cell-specific gross and net photosynthesis rates), statistical tests were performed with only data corresponding to the highest light intensity used, i.e. 400 µmol photons m^{-2} s^{-1} for intact-, whole coral measurements, and 480 µmol photons m^{-2} s^{-1} for microsensor measurements.

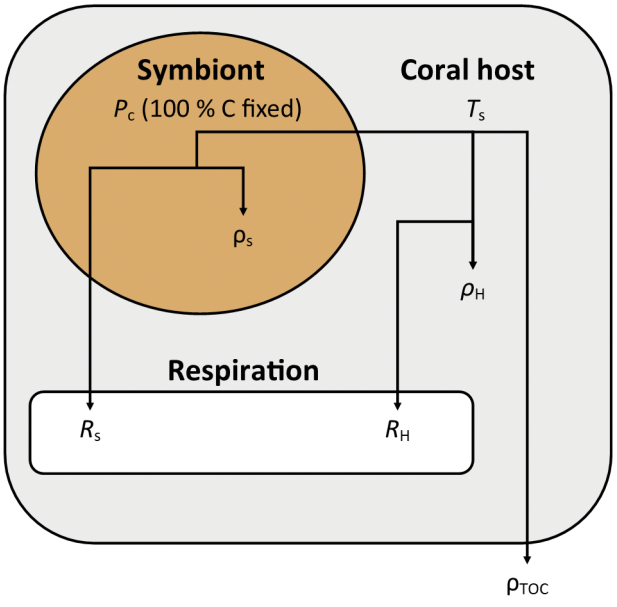

Fig. 1. Overview of photosynthate translocation and the carbon budget overall. P_c: total amount of inorganic C fixed through photosynthesis, hence 100% fixed for all treatments and time points (see Table 1 for detailed data); T_s: C translocated from symbiont to coral host; ρ: C incorporated into the symbionts (ρ_s) and coral host (ρ_H); R: C used for respiration by symbionts (R_s) and by the coral host (R_H); ρ_{TOC}: total amount of C lost from the holobiont as organic carbon

3. RESULTS

The current study focuses on carbon energy budgets established with ^{13}C-isotope tracer experiments and determination of O_2 fluxes at both the micro- and macroscale. Additional results on radiative energy budgets, temperature dynamics, light microenvironments, chlorophyll content, and symbiont density can be found in Lyndby et al. (2019).

3.1. Photosynthesis vs. irradiance curves

We observed an initial difference in areal gross photosynthesis between fed and unfed corals measured at the microscale, as production initially increased in fed corals at the onset of thermal stress, whereas production decreased in unfed corals (compare fed T_0 to fed T_1, and unfed T_0 to unfed T_1 in Fig. 2a,b). Feeding status had a significant effect on areal gross photosynthesis measured with microsensors (ANOVA, $F_{1,30}$ = 6.0, p = 0.020); however, heat stress did not affect areal gross photosynthesis significantly (ANOVA, $F_{1,30}$ = 0.1, p = 0.749), and no significant interaction was found between feeding status and heat stress (ANOVA, $F_{1,30}$ = 2.6, p = 0.114). A Tukey post hoc analysis showed that fed corals had a significantly higher production after onset of heat stress compared to unfed corals (i.e. fed T_1 vs. unfed T_1; p = 0.034). Additionally, we found a significant effect of heat stress on fed coral areal gross photosynthesis on a microscale when including the last time point (i.e. T_0 vs. T_1 vs. T_2; ANOVA, $F_{2,19}$ = 4.1, p = 0.030), although a Tukey post hoc analysis showed that only fed corals exposed to heat stress were significantly different (i.e. T_1 vs. T_2; p = 0.027), while control corals were not significantly different from any of the heat-stressed corals (p > 0.05 for both T_0 vs. T_1 and T_0 vs. T_2).

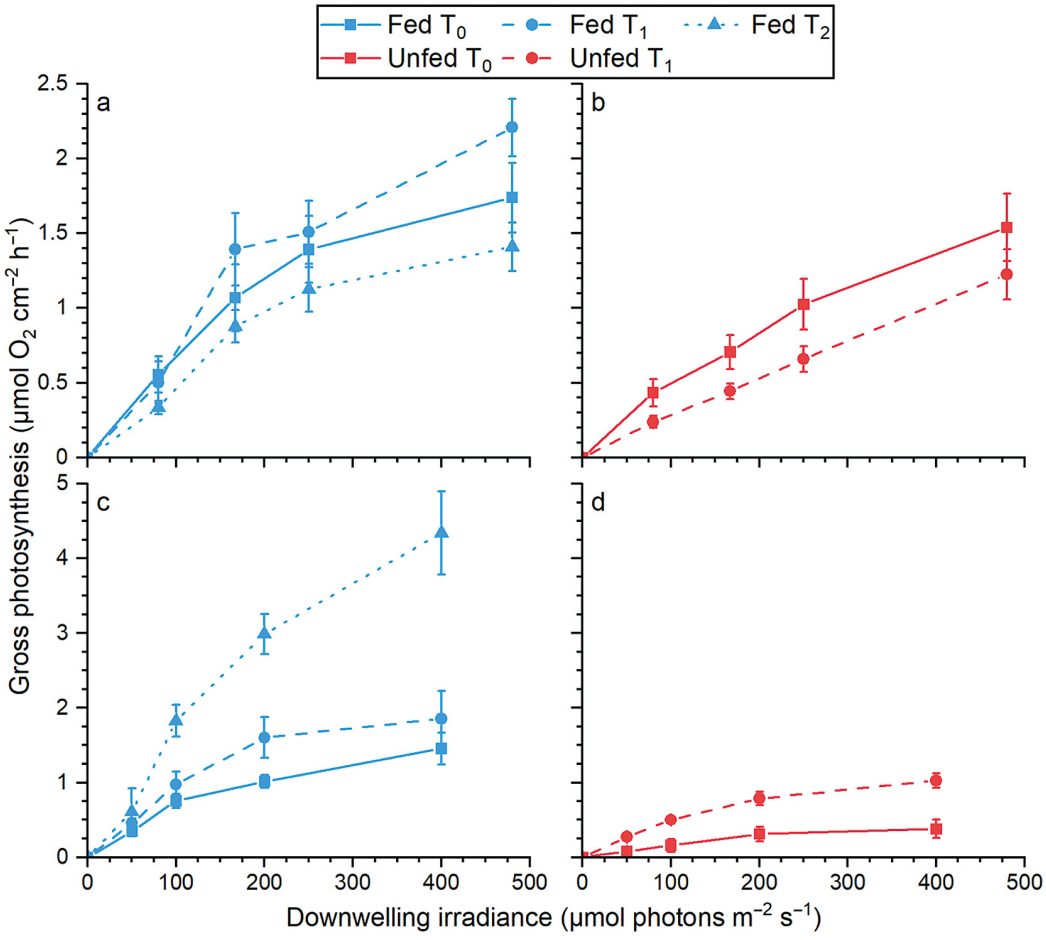

Fig. 2. Gross O_2 production in *Pocillopora damicornis* as a function of increasing photon irradiance as measured with (a,b) O_2 microsensors on a polyp scale and (c,d) O_2 gas exchange measurements of whole coral fragments. Measurements were performed on (a,c) corals fed daily and (b,d) unfed corals for each of 3 temperature treatments: T_0 (control, solid lines), T_1 (3 d at 30°C; dashed lines), and T_2 (8 d at 30°C; dotted lines). Symbols with error bars represent mean ± SEM (n = 5–12)

Unlike areal gross photosynthesis on a microscale, the production measured on a macroscale (whole corals) increased with thermal stress in both fed and unfed corals (T_0 vs. T_1; Fig. 2c,d). Both heat stress (ANOVA, $F_{1,14}$ = 4.7, p = 0.048) and feeding status (ANOVA, $F_{1,14}$ = 15.5, p < 0.01) had a significant effect on the areal gross photosynthesis on a macroscale. However, we found no significant interaction between heat stress and feeding status on a macroscale (ANOVA, $F_{1,14}$ = 0.2, p = 0.60). Tukey post hoc analysis showed that control corals were significantly different from each other (i.e. fed T_0 vs. unfed T_0; p = 0.043), but no difference was found comparing heat-stressed fed and unfed corals (fed T_1 vs. unfed T_1; p = 0.09). Additionally, we found a significant effect of heat stress on fed corals including all time points (T_0 vs. T_1 vs. T_2; ANOVA, $F_{2,11}$ = 13.5, p < 0.01). Tukey post hoc analysis showed that after 13 d of heat stress, fed corals were significantly different from both control corals (T_2 vs. T_0; p < 0.01) and fed corals after 8 d of heat stress (T_2 vs. T_1; p < 0.01).

With gas-exchange measurements of areal net photosynthesis, we found a compensation irradiance (i.e. the irradiance above which net O_2 production is observed) of >100 µmol photons m^{-2} s^{-1} in fed corals at both micro- and macroscale measurements (Fig. 3a,c). In contrast, the compensation irradiance for unfed corals was >200 µmol photons m^{-2} s^{-1} (Fig. 3b,d). The combination of thermal stress and starvation increased the compensation irradiance to 250 µmol photons m^{-2} s^{-1} at T_0, and 480 µmol photons m^{-2} s^{-1} at T_1 on a microscale, and 200 µmol photons m^{-2} s^{-1} at T_0–T_1 on a macroscale (Fig. 3b,d). Relative to macroscale measurements, microscale light respiration was enhanced for fed and unfed corals (Fig. 3a,b). Coral dark respiration was similar for all treatments except for fed corals at T_2 (Fig. 3c), which showed a 400% increase in O_2 consumption compared to fed corals at T_0 (0.6 ± 0.04 vs. 2.4 ± 0.28 µmol O_2 cm^{-2} h^{-1}).

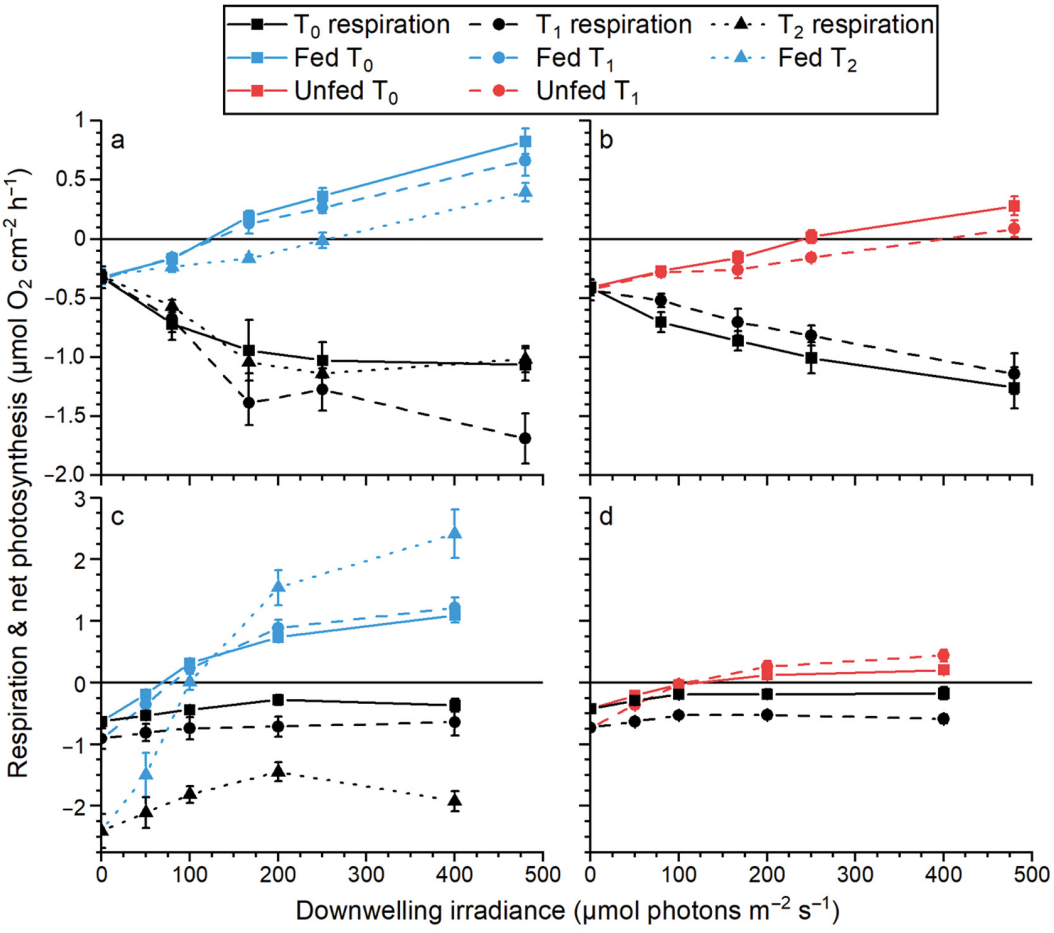

Fig. 3. As in Fig. 2, but for net O_2 production and consumption (respiration) in *Pocillopora damicornis* as a function of increasing downwelling photon irradiance. Symbols with error bars represent means ± SEM (n = 12)

3.2. Cell-specific O_2 flux for *Cladocopium*

Cell-specific gross photosynthesis measured on intact corals (cells *in vivo*; Fig. 4a) showed a clear trend of increasing production per cell with increasing light intensity, with the greatest increase observed with cells from heat-stressed corals (fed T_2; Fig. 4a). Heat stress significantly affected cell-specific gross photosynthesis rates (ANOVA, $F_{1,14}$ = 22.0, p << 0.01), while feeding status did not affect production (ANOVA, $F_{1,14}$ = 0.2, p = 0.670). However, a significant interaction was found between heat stress and feeding status (ANOVA, $F_{1,14}$ = 5.9, p = 0.029). Furthermore, we found that heat stress had a significant effect on cell specific gross photosynthesis in cells from fed corals including all time points (T_0 vs. T_1 vs. T_2; ANOVA, $F_{2,11}$ = 32.1, p << 0.01), and Tukey post hoc analysis showed that cell-specific gross photosynthesis in cells after 13 d of heat stress was significantly higher than the production in fed control corals (T_2 vs. T_0; p << 0.01) and fed corals after 8 d of stress (T_2 vs. T_1; p << 0.01).

Unlike *in vivo* cell-specific gross photosynthesis, the cell-specific gross photosynthesis rates measured on freshly isolated symbionts (*in vitro*) did not show any sign of increasing production with increased irradiance (Fig. 4b), and we found no significant effect of heat stress (ANOVA, $F_{1,8}$ = 3.6, p = 0.096) or feeding status (ANOVA, $F_{1,8}$ = 5.2, p = 0.051) on the cell-specific gross photosynthesis in freshly isolated symbionts.

3.3. Carbon budget of entire coral fragments

The total inorganic carbon assimilation (P_c in µg C cm^{-2} h^{-1}) increased with thermal stress in fed corals, resulting in a 58 % increase from T_0 to T_1 and a 195 % increase from T_0 to T_2 from a baseline of 11.05 µg C

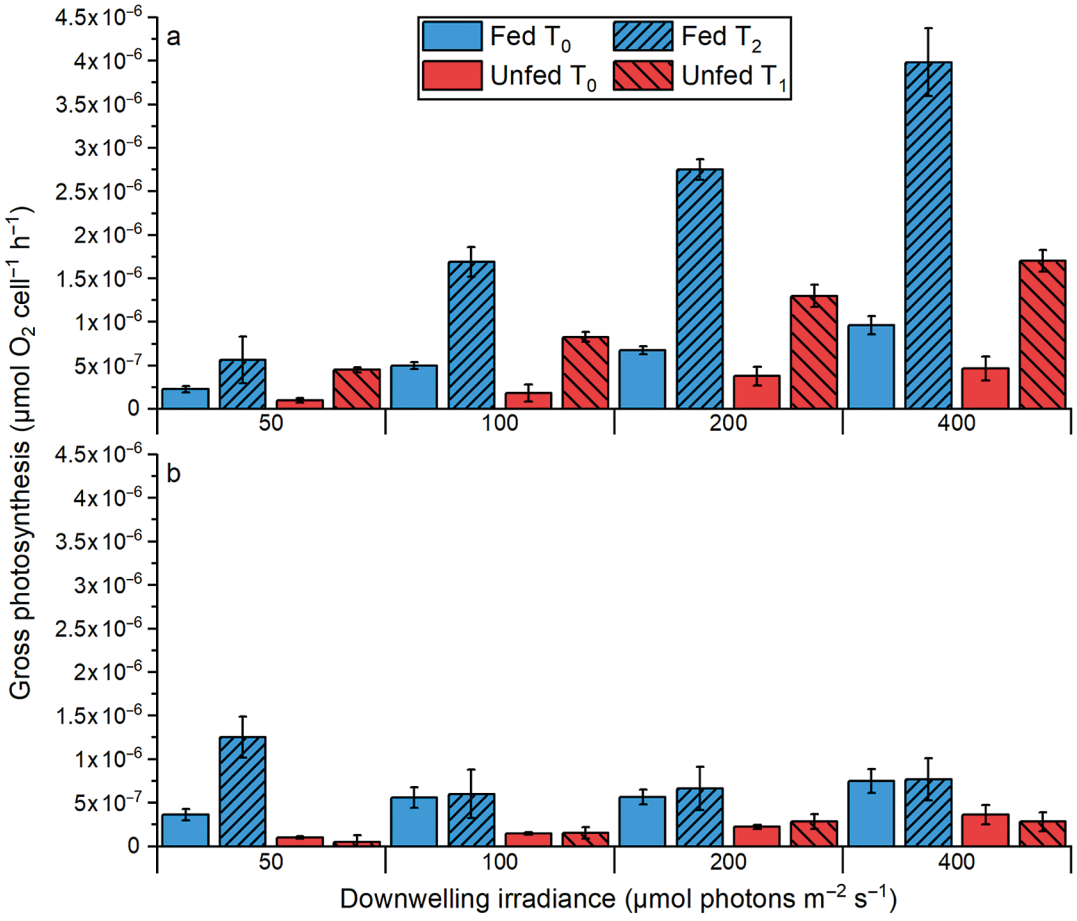

Fig. 4. Cell-specific gross photosynthetic O_2 production rates as a function of incident photon irradiance measured on (a) intact fragments of fed and unfed *Pocillopora damicornis* (*in vivo*) and (b) freshly isolated *Cladocopium* from *P. damicornis* (*in vitro*) at increasing exposure time to heat stress. Blue columns represent measurements on fed corals, and red columns measurements on unfed corals. Data are means ± SEM (n = 3–5)

cm^{-2} h^{-1} in fed corals, and a 161% increase from T_0 to T_1 from 3.36 µg C cm^{-2} h^{-1} in unfed corals. Both heat stress (ANOVA, $F_{1,14}$ = 10.0, $p < 0.01$) and feeding status (ANOVA, $F_{1,14}$ = 19.3, $p \ll 0.01$) had a significant effect on P_c, although the interaction between feeding status and heat stress was not significant (ANOVA, $F_{1,14}$ = 0.1, p = 0.79). We found a significant effect of heat stress for fed corals (ANOVA, $F_{2,11}$ = 17.58, $p \ll 0.01$), but Tukey post hoc analyses showed that only T_2 was significantly different from both T_0 ($p \ll 0.01$) and T_1 ($p < 0.01$).

Carbon translocation rates (T_s in % fixed carbon) from symbiont to host showed a slight increase during heat stress for all treatments (85.8% at T_0 vs. 93.7% at $T_{1\text{-}2}$; Table 1), while the respiration rate (R_s in % fixed carbon) of symbionts in hosts decreased and host respiration (R_H) increased with thermal stress (Table 1). The carbon incorporation rates were generally low for both symbionts (ρ_s) and hosts (ρ_H) in all treatments as compared to other assessed coral species (Tremblay et al. 2016), and the rates decreased with thermal stress.

We found that both heat stress (ANOVA, $F_{1,12}$ = 25.5, $p \ll 0.01$) and feeding status (ANOVA, $F_{1,12}$ = 53.2, $p \ll 0.01$) had a significant effect on carbon incorporation rates of the coral host (ρ_H). We additionally found a significant interaction between feeding status and heat stress (ANOVA, $F_{1,12}$ = 28.8, $p \ll 0.01$), and Tukey post hoc analyses showed that control coral hosts (i.e. T_0 fed vs. T_0 unfed), as well as fed hosts (i.e. T_0 fed vs. T_1 fed) were both significantly different ($p \ll 0.01$); however, differences between unfed hosts (i.e. T_0 unfed vs. T_1 unfed; p = 0.99) and heat-stressed hosts (T_1 fed vs. T_1 unfed; p = 0.55) were not significant. Furthermore, we found a significant effect of heat stress on fed coral host ρ_H (T_0 vs. T_1 vs. T_2; ANOVA, $F_{2,9}$ = 17.9, $p \ll 0.01$), while Tukey post hoc analyses only found that control hosts (i.e. T_0 fed) differed from T_1 ($p \ll 0.01$) and T_2 ($p < 0.01$) hosts.

Similar to hosts, we found that both heat stress (ANOVA, $F_{1,12}$ = 7.7, $p < 0.05$) and feeding status (ANOVA, $F_{1,12}$ = 36.6, $p << 0.01$) had a significant effect on carbon incorporation rates in symbionts (ρ_s). Additionally, we found a significant interaction between feeding status and heat stress (ANOVA, $F_{1,12}$ = 5.2, $p < 0.05$). Tukey post hoc analyses showed that symbionts from fed corals (i.e. T_0 fed vs. T_1 fed; $p < 0.05$), as well as symbionts from heat-stressed corals (i.e. T_1 fed vs. T_1 unfed; $p \ll 0.01$) were significantly different, while symbionts from control corals (T_0 fed vs. T_0 unfed; p = 0.08) and symbionts from unfed corals (T_0 unfed vs. T_1 unfed; p = 0.98) were not. Furthermore, we found a significant effect of heat stress when including all time points for symbionts from fed corals (T_0 vs. T_1 vs. T_2; ANOVA, $F_{2,9}$ = 6.58, $p < 0.05$). Tukey post hoc analyses showed that symbionts at T_1 differed from symbionts at T_0 and T_2 ($p < 0.05$ for both).

Finally, carbon lost from the system, calculated as lost organic carbon (ρ_{TOC} of % fixed carbon), was estimated from the total carbon budget with control fed corals on average excreting 540% more carbon as organic waste than control unfed corals (8.32 µg C cm^{-2} h^{-1} for fed and 1.54 µg C cm^{-2} h^{-1} for unfed corals).

4. DISCUSSION

In this study, we estimated the mass-balanced autotrophic carbon budgets in fed and heterotrophically starved *Pocillopora damicornis* corals. The aim was to compare allocation of resources depending on feeding status and to investigate how holobionts with different nutritional states respond to thermal stress (Table 1). We also assessed how different coral com-

Table 1. Mass balance of photosynthate translocation and carbon budget for fed and unfed *Pocillopora damicornis* as a function of time under heat stress. Incorporation rates of carbon are based on ^{13}C-isotope incubation experiments using a pulse period of 4 h. See Fig. 1 for a schematic overview of the carbon budget and abbreviations used. Values are %, and data in parentheses represent means ± SEM (n = 3–5) (µg C cm^{-2} h^{-1}). Note that T_s, R_H, and ρ_{TOC} values do not include SEM, as they are calculated from mean values of the other factors. For details on the calculations, see Tremblay et al. (2012)

	Fed T_0	Fed T_1	Fed T_2	Unfed T_0	Unfed T_1
P_c	100 (11.05 ± 0.93)	100 (17.46 ± 2.96)	100 (32.59 ± 2.89)	100 (3.36 ± 1.07)	100 (8.77 ± 0.93)
ρ_s	0.11 (0.012 ± 0.002)	0.13 (0.022 ± 0.002)	0.03 (0.011 ± 0.002)	0.11 (0.004 ± 0.002)	0.05 (0.005 ± 0.002)
R_s	13.96 (1.54 ± 0.78)	6.42 (1.12 ± 0.07)	6.91 (2.25 ± 0.76)	14.15 (0.47 ± 0.80)	5.30 (0.46 ± 0.07)
T_s	85.93 (9.50)	93.45 (16.32)	93.06 (30.33)	85.74 (2.88)	94.64 (8.30)
ρ_H	0.60 (0.067 ± 0.006)	0.15 (0.03 ± 0.002)	0.11 (0.04 ± 0.005)	0.50 (0.02 ± 0.002)	0.21 (0.02 ± 0.004)
R_H	10.09 (1.12)	32.83 (5.73)	35.68 (11.63)	39.33 (1.32)	52.17 (4.57)
ρ_{TOC}	75.24 (8.32)	60.47 (10.56)	57.27 (18.66)	45.91 (1.54)	42.27 (3.71)

partments modulate respiration at the macro- and microscale when subjected to different feeding, temperature, and light regimes. Measurements in this study were performed in parallel with Lyndby et al. (2019), who established closed radiative energy budgets for the same coral specimens. Lyndby et al. (2019) argued that fed corals harbored a symbiont population that sustained high photosynthetic rates for an extended period during thermal stress, which subsequently would increase the resistance of the coral holobiont to bleaching (cf. Fig. 10 in Lyndby et al. 2019). Here, we provide further insights as to why coral feeding increases the resistance to thermal stress.

Before onset of thermal stress, the amount of fixed inorganic carbon (P_c) was ~3.3-fold higher in fed corals compared to unfed corals. Furthermore, the photosynthetic activity of fed and unfed corals (Figs. 2c,d & 3c,d) showed clear differences between treatments, with fed control corals (T_0) exhibiting a ~5-fold higher O_2 production. This corresponded well with enhanced symbiont cell densities, which were 2-fold enhanced for fed vs. unfed corals (Fig. 3a in Lyndby et al. 2019). Overall, and as previously observed (Borell et al. 2008, Ferrier-Pagès et al. 2010), feeding increased the photosynthetic performances of both the holobiont and of the individual symbionts.

Host respiration (R_H) as well as the release of organic carbon (ρ_{TOC}; presumably in the form of mucus) also differed substantially between fed and unfed control corals. While the amount of carbon respired was similar between treatments (1.1–1.3 µg C cm^{-2} h^{-1}), the proportion of initial fixed carbon was almost 4-fold lower for unfed corals, which thus respired almost 40% of their initially fixed carbon. In contrast, fed corals only respired ~10% of the initially fixed carbon. Thus, although fed and unfed holobionts have similar respiration rates, the sources of respired carbon are different. Unfed corals exclusively respired autotrophically acquired carbon, while fed corals mostly respired heterotrophically acquired carbon. As a consequence, fed corals excreted on average >5 times more organic carbon than unfed corals. Such preferential use of heterotrophic carbon for the respiratory needs of fed corals suggests that this source is either more energy rich, easier to consume than the autotrophic source, or its respiration is needed to free the nitrogen and phosphorus molecules contained in the food and thus is essential for corals. Alternatively, the respiration of heterotrophic food also increases the intracellular pool of dissolved inorganic carbon (CO_2), thereby enhancing rates of symbiont photosynthesis. In free-living algae, mixotrophic conditions showed enhanced glycolysis, photosynthetic carbon fixation, and pentose phosphate pathways (and thus more ATP, carbon skeleton structure, and NADPH) than autotrophic conditions (Li et al. 2020). The same might apply to the coral–dinoflagellate symbiosis, although this remains to be tested.

Corals are counted among the most efficient aquatic photosynthetic organisms (Al-Najjar et al. 2010, Brodersen et al. 2014, Lichtenberg et al. 2017), and the high photosynthetic activity of *P. damicornis* observed here and in Lyndby et al. (2019) supports that notion. However, carbon energy budgets established here show evidence that a large fraction of assimilated carbon is lost quickly, either as respiration or released as dissolved inorganic carbon, in agreement with a previous study on energy and carbon dynamics in *P. eydouxi* (Davies 1984). Released carbon can act as a food source for surface-associated microbes (Bourne & Munn 2005, Thompson et al. 2015) that may confer benefits to the coral holobionts, e.g. in terms of increased resistance to heat stress (Rosenberg et al. 2007) or nutrient supply via fixed nitrogen from diazotrophs being translocated to the coral host (Grover et al. 2003, Bednarz et al. 2017, Pupier et al. 2019). The majority of autotrophically acquired carbon is respired and used for daily household metabolism that covers up to 95% of a coral's daily metabolic energy demand (Davies 1984, Muscatine et al. 1984, Edmunds & Davies 1986). For fast-growing corals like *P. damicornis*, a large fraction of the CO_2 and energy derived from respiration is used for the calcification process, and might explain the high respiration rates measured here (Furla et al. 2000). As a consequence, the amount of carbon actually being incorporated into symbionts (ρ_s) and host (ρ_H) was low. Symbionts extracted from control corals from both feeding groups incorporated 0.1% of initially fixed carbon for themselves, and incorporation of carbon into hosts was similarly low, although ~5-fold higher in hosts compared to their symbionts (Table 1). In contrast, a previous study found several orders of magnitude higher incorporation rates (15–30% of initially fixed carbon, depending on incubation time) for the branching coral *Stylophora pistillata*, a close relative of *P. damicornis*, suggesting species specificity as an important factor (Tremblay et al. 2012). Low carbon assimilation rates in coral tissue may occur when other nutrients, such as nitrogen or phosphorus, are limiting coral and symbiont growth (Falkowski et al. 1984, Rosset et al. 2017). The seawater received in the incubation aquaria was oligotrophic (<0.5 µM nitrogen and <0.2 µM phosphorus), and nutrient limitation might thus explain

the low assimilation rates of *P. damicornis* in our study (Table 1). This assumption is further supported by the enhanced photosynthate incorporation rates of fed vs. unfed corals (3–4 times higher assimilation in both tissue and symbionts for fed corals), together strongly suggesting that carbon assimilation was limited by nutrient availability.

Finally, measurements of gross O_2 production rates of isolated symbionts were about 1 order of magnitude lower than the gross O_2 production rates estimated from *in vivo* measurements on intact corals (Fig. 4). This suggests that the symbionts benefit from properties of the animal tissue and skeleton, e.g. through optimized light exposure and potentially other host-mediated factors including pH, nutrients, or spectral filtering by host pigments, leading to enhanced *in vivo* photosynthetic efficiency (Enriquez et al. 2005, Wangpraseurt et al. 2019). Although both *in vivo* and *in vitro* measurements were performed under similar levels of incident photon scalar irradiance, the actual scalar irradiance will differ between the 2 measurements because of light scattering in the coral tissue and skeleton (Wangpraseurt et al. 2012, 2014, 2019). However, inorganic nutrient supply from the coral host (e.g. NH_4^+), as well as organic carbon supply through heterotrophy, can also contribute to the observed enhancement of photosynthetic efficiency *in vivo* (Borell & Bischof 2008, Hoadley et al. 2016).

Thermal stress significantly decreased symbiont density per area (Fig. 3b in Lyndby et al. 2019), while values of chlorophyll $a+c_2$ per cell and per tissue area remained similar (Fig. 3c in Lyndby et al. 2019). In addition, short-term thermal stress had a positive effect on the amount of inorganic carbon fixed for both fed and unfed corals, and both treatments nearly tripled the assimilation at the end of the experiment (compare P_c for T_0 to $T_{1\text{-}2}$ in Table 1). Although radiative energy budgets showed that photosynthetic performance decreased by the end of the experiment, cell-specific gross photosynthesis was found to increase with thermal stress (see Fig. 6b in Lyndby et al. 2019). This supports earlier observations of bleaching corals undergoing an optical feedback loop (Enriquez et al. 2005, Wangpraseurt et al. 2017), which can involve enhanced photosynthesis of remaining symbionts during initial bleaching. Despite increased carbon fixation at high temperatures, the amount of incorporated carbon remained unchanged for symbionts at 0.011 and 0.005 µg C cm^{-2} h^{-1} for fed and unfed corals, respectively, by the end of the experiment (compare ρ_s for T_0 to $T_{1\text{-}2}$ in Table 1), although resulting in an overall lower proportion of initially fixed carbon retained by the symbionts during thermal stress. Similarly, unfed corals incorporated the same amount of carbon by the end of the experiment, while fed corals showed a decrease of ~40% in the amount of carbon taken up at T_2 compared to control corals (decrease from 0.07 to 0.04 µg C cm^{-2} h^{-1}). Additionally, translocation rates and respiration in coral hosts greatly increased with thermal stress, thus suggesting that a lowered proportion of incorporated carbon in both symbionts and hosts acted as compensation to thermal stress observed as increased respiration rates in both feeding treatments.

The O_2 fluxes measured at the macro- and microscale were found to differ in previous studies (e.g. Schrameyer et al. 2014), and it was shown that gross photosynthesis is underestimated when calculated from net O_2 fluxes on whole fragments. The underestimation of macroscale gross photosynthesis estimates is due to the assumption that dark respiration is representative of light respiration (Schrameyer et al. 2014, and Eq. 2). The results obtained here show that respiration rates in control corals were higher on the microscale compared to the macroscale, as found in earlier studies (e.g. Schrameyer et al. 2014), while P_n rates were similar at both scales (Fig. 3). Such disparity naturally resulted in an overall higher P_g at the microscale for both feeding treatments compared to the macroscale measurements (T_0–T_1 in Fig. 2a,c). However, at the end of the experiment (T_2), this was inverted, as P_g on a macroscale was ~3-fold higher compared to microscale measurements. Our microscale measurements were restricted to few, individual polyps, oriented at a defined angle near the apical tips of the coral branch, which could potentially underestimate the productivity of polyp areas that were not assessed with microsensor measurements. The difference between micro- and macroscale measurements for fed corals at T_2 (Fig. 2a,c) indicates that photosynthesis was heterogeneously distributed over the coral surface (Al-Horani et al. 2005). In other words, thermal stress affected symbiont photosynthesis differently depending on their location in coral tissue. Scalar irradiance measurements on bare skeletons of *P. damicornis* (Fig. A2) revealed that light exposure near the base of the coral branch was increased by about 100% compared to the apical branch tip. Previous studies on spatial distribution of photosynthesis across the coral tissue surface revealed that the majority of photosynthetic activity is located around the tissue covering the corallite septa, with up to 1 order of magnitude increased photosynthesis compared to adjacent coenosarc tissue (Al-Horani et al. 2005). These findings empha-

size the potential underestimation of the photosynthetic activity of the polyp regions near the base of the coral branch. The enhanced O_2 production observed for macroscale measurements of fed corals at T_2 may thus be additionally affected by the backscattering properties in polyp areas around the base of the coral branch, as fed corals at T_2 had reduced cell density compared to controls (T_0; Fig. 3a in Lyndby et al. 2019), which caused an enhanced radiative exposure of the symbionts residing in the deeper tissue layers, thus leading to an overall increased O_2 production.

Coral metabolism and the metabolic interactions between host and symbionts in times of stress is receiving increasing attention due to anthropogenic climate change threatening coral reefs globally. By establishing mass balanced carbon budgets, we showed how heterotrophically fed and starved corals respond to short-term thermal stress, and how different feeding status can affect coral thermal resistance. Additionally, we established radiative energy budgets for the same coral colonies (Lyndby et al. 2019). We found that overall trends for the implications of heterotrophy on thermal resistance is similar with the 2 budgets established, and that combining the 2 methods greatly increases the level of detail on how corals respond to thermal stress that would otherwise be hidden when using only one method.

The results obtained in this study, together with previous results on coral heterotrophy, suggest that corals with the ability to increase heterotrophy, or living in plankton-rich areas, will have a better chance to survive environmental changes. For example, turbid environments with attenuated levels of solar irradiance and high organic matter content supporting elevated coral heterotrophy have been shown to protect corals from severe bleaching during heat waves (Morgan et al. 2017, Van Woesik & McCaffrey 2017). More research, e.g. using modern remote sensing technology, is needed to identify reef locations with high zooplankton concentrations. Also, more research should aim at identifying which corals are the most heterotrophic species; not all coral species have the same heterotrophic capacities or can increase heterotrophy during environmental stress (Ferrier-Pagès et al. 2010). Finally, future studies should aim to determine the role of heterotrophy on stress resistance under repeated stress scenarios, such as repeated bleaching events. The above knowledge will help to identify priorities for reef conservation, such as targeting species with high heterotrophic activity, or locations for reef restoration with a high availability of zooplankton.

Acknowledgements. We thank the staff at the Scientific Center of Monaco for their excellent assistance with experimental procedures and labor-intensive general maintenance and care of the corals for the duration of this study. We also thank Sofie Jakobsen for logistic help with experimental equipment. The study was funded by grants from the Carlsberg Foundation (D.W., M.K.), European Union's Horizon 2020 research and innovation program (D.W.), the Independent Research Fund Denmark (M.K.), the Gordon and Betty Moore Foundation (M.K.; Grant no. GBMF9206, https://doi.org/10.37807/GBMF9206) and the Scientific Center of Monaco (part of the RTPI Nutress).

LITERATURE CITED

Al-Horani FA, Ferdelman T, Al-Moghrabi SM, de Beer D (2005) Spatial distribution of calcification and photosynthesis in the scleractinian coral *Galaxea fascicularis.* Coral Reefs 24:173–180

Al-Najjar MA, de Beer D, Jørgensen BB, Kühl M, Polerecky L (2010) Conversion and conservation of light energy in a photosynthetic microbial mat ecosystem. ISME J 4: 440–449

Anthony KRN, Fabricius KE (2000) Shifting roles of heterotrophy and autotrophy in coral energetics under varying turbidity. J Exp Mar Biol Ecol 252:221–253

Bednarz VN, Grover R, Maguer JF, Fine M, Ferrier-Pagès C (2017) The assimilation of diazotroph-derived nitrogen by scleractinian corals depends on their metabolic status. MBio 8:e02058-16

Borell EM, Bischof K (2008) Feeding sustains photosynthetic quantum yield of a scleractinian coral during thermal stress. Oecologia 157:593–601

Borell EM, Yuliantri AR, Bischof K, Richter C (2008) The effect of heterotrophy on photosynthesis and tissue composition of two scleractinian corals under elevated temperature. J Exp Mar Biol Ecol 364:116–123

Bourne DG, Munn CB (2005) Diversity of bacteria associated with the coral *Pocillopora damicornis* from the Great Barrier Reef. Environ Microbiol 7:1162–1174

Brodersen KE, Lichtenberg M, Ralph PJ, Kühl M, Wangpraseurt D (2014) Radiative energy budget reveals high photosynthetic efficiency in symbiont-bearing corals. J R Soc Interface 11:20130997

Brown BE (1997) Coral bleaching: causes and consequences. Coral Reefs 16:S129–S138

Courtial L, Roberty S, Shick JM, Houlbrèque F, Ferrier-Pagès C (2017) Interactive effects of ultraviolet radiation and thermal stress on two reef-building corals. Limnol Oceanogr 62:1000–1013

Davies PS (1984) The role of zooxanthellae in the nutritional energy requirements of *Pocillopora eydouxi.* Coral Reefs 2:181–186

Edmunds PJ, Davies PS (1986) An energy budget for *Porites porites* (Scleractinia). Mar Biol 92:339–347

Enriquez S, Méndez ER, Iglesias-Prieto R (2005) Multiple scattering on coral skeletons enhances light absorption by symbiotic algae. Limnol Oceanogr 50:1025–1032

Falkowski PG, Dubinsky Z, Muscatine L, Porter JW (1984) Light and the bioenergetics of a symbiotic coral. Bioscience 34:705–709

Ferrier-Pagès C, Rottier C, Beraud E, Levy O (2010) Experimental assessment of the feeding effort of three scleractinian coral species during a thermal stress: effect on the

rates of photosynthesis. J Exp Mar Biol Ecol 390:118–124
Furla P, Galgani I, Durand I, Allemand D (2000) Sources and mechanisms of inorganic carbon transport for coral calcification and photosynthesis. J Exp Biol 203:3445–3457
Gardner SG, Raina JB, Ralph PJ, Petrou K (2017) Reactive oxygen species (ROS) and dimethylated sulphur compounds in coral explants under acute thermal stress. J Exp Biol 220:1787–1791
Godinot C, Ferrier-Pagès C, Sikorski S, Grover R (2013) Alkaline phosphatase activity of reef-building corals. Limnol Oceanogr 58:227–234
Grottoli AG, Rodrigues LJ, Palardy JE (2006) Heterotrophic plasticity and resilience in bleached corals. Nature 440: 1186–1189
Grover R, Maguer JF, Allemand D, Ferrier-Pagès C (2003) Nitrate uptake in the scleractinian coral *Stylophora pistillata*. Limnol Oceanogr 48:2266–2274
Hoadley KD, Pettay DT, Dodge D, Warner ME (2016) Contrasting physiological plasticity in response to environmental stress within different cnidarians and their respective symbionts. Coral Reefs 35:529–542
Hoegh-Guldberg O, Poloczanska ES, Skirving W, Dove S (2017) Coral reef ecosystems under climate change and ocean acidification. Front Mar Sci 4:158
Hoogenboom M, Beraud E, Ferrier-Pagès C (2010) Relationship between symbiont density and photosynthetic carbon acquisition in the temperate coral *Cladocora caespitosa*. Coral Reefs 29:21–29
Houlbrèque F, Ferrier-Pagès C (2009) Heterotrophy in tropical scleractinian corals. Biol Rev Camb Philos Soc 84:1–17
Houlbrèque F, Tambutté E, Richard C, Ferrier-Pagès C (2004) Importance of a micro-diet for scleractinian corals. Mar Ecol Prog Ser 282:151–160
Hughes AD, Grottoli AG (2013) Heterotrophic compensation: a possible mechanism for resilience of coral reefs to global warming or a sign of prolonged stress? PLOS ONE 8:e81172
Hughes AD, Grottoli AG, Pease TK, Matsui Y (2010) Acquisition and assimilation of carbon in non-bleached and bleached corals. Mar Ecol Prog Ser 420:91–101
Hughes TP, Kerry JT, Álvarez-Noriega M, Álvarez-Romero JG and others (2017) Global warming and recurrent mass bleaching of corals. Nature 543:373–377
Jacobson LM, Edmunds PJ, Muller EB, Nisbet RM (2016) The implications of reduced metabolic rate in resource-limited corals. J Exp Biol 219:870–877
Kühl M, Cohen Y, Dalsgaard T, Jørgensen BB, Revsbech NP (1995) Microenvironment and photosynthesis of zooxanthellae in scleractinian corals studied with microsensors for O_2, pH and light. Mar Ecol Prog Ser 117:159–172
Kühl M, Glud RN, Ploug H, Ramsing NB (1996) Microenvironmental control of photosynthesis and photosynthesis-coupled respiration in an epilithic cyanobacterial biofilm. J Phycol 32:799–812
LaJeunesse TC, Parkinson JE, Gabrielson PW, Jeong HJ, Reimer JD, Voolstra CR, Santos SR (2018) Systematic revision of Symbiodiniaceae highlights the antiquity and diversity of coral endosymbionts. Curr Biol 28: 2570–2580.e6
Lesser MP (1996) Elevated temperatures and ultraviolet radiation cause oxidative stress and inhibit photosynthesis in symbiotic dinoflagellates. Limnol Oceanogr 41: 271–283
Li T, Yang F, Xu J, Wu H, Mo J, Dai L, Xiang W (2020) Evaluating differences in growth, photosynthetic efficiency, and transcriptome of *Asterarcys* sp. SCS-1881 under autotrophic, mixotrophic, and heterotrophic culturing conditions. Algal Res 45:101753
Lichtenberg M, Brodersen KE, Kuhl M (2017) Radiative energy budgets of phototrophic surface-associated microbial communities and their photosynthetic efficiency under diffuse and collimated light. Front Microbiol 8:452
Lyndby NH, Holm JB, Wangpraseurt D, Ferrier-Pagès C, Kühl M (2019) Bio-optical properties and radiative energy budgets in fed and unfed scleractinian corals (*Pocillopora* sp.) during thermal bleaching. Mar Ecol Prog Ser 629:1–17
Morgan KM, Perry CT, Johnson JA, Smithers SG (2017) Nearshore turbid-zone corals exhibit high bleaching tolerance on the Great Barrier Reef following the 2016 ocean warming event. Front Mar Sci 4:224
Muscatine L, Cernichiari E (1969) Assimilation of photosynthetic products of zooxanthellae by a reef coral. Biol Bull (Woods Hole) 137:506–523
Muscatine L, McCloskey LR, Marian RE (1981) Estimating the daily contribution of carbon from zooxanthellae to coral animal respiration. Limnol Oceanogr 26:601–611
Muscatine L, Falkowski PG, Porter JW, Dubinsky Z (1984) Fate of photosynthetic fixed carbon in light- and shade-adapted colonies of the symbiotic coral *Stylophora pistillata*. Proc R Soc B 222:181–202
Palardy JE, Rodrigues LJ, Grottoli AG (2008) The importance of zooplankton to the daily metabolic carbon requirements of healthy and bleached corals at two depths. J Exp Mar Biol Ecol 367:180–188
Pupier CA, Bednarz VN, Grover R, Fine M, Maguer JF, Ferrier-Pagès C (2019) Divergent capacity of scleractinian and soft corals to assimilate and transfer diazotrophically derived nitrogen to the reef environment. Front Microbiol 10:1860
Revsbech NP, Jørgensen BB (1983) Photosynthesis of benthic microflora measured with high spatial resolution by the oxygen microprofile method: capabilities and limitations of the method. Limnol Oceanogr 28:749–756
Rodrigues LJ, Grottoli AG (2007) Energy reserves and metabolism as indicators of coral recovery from bleaching. Limnol Oceanogr 52:1874–1882
Rosenberg E, Koren O, Reshef L, Efrony R, Zilber-Rosenberg I (2007) The role of microorganisms in coral health, disease and evolution. Nat Rev Microbiol 5:355–362
Rosset S, Wiedenmann J, Reed AJ, D'Angelo C (2017) Phosphate deficiency promotes coral bleaching and is reflected by the ultrastructure of symbiotic dinoflagellates. Mar Pollut Bull 118:180–187
Schrameyer V, Wangpraseurt D, Hill R, Kühl M, Larkum AWD, Ralph PJ (2014) Light respiratory processes and gross photosynthesis in two scleractinian corals. PLOS ONE 9:e110814
Sebens KP, Vandersall KS, Savina LA, Graham KR (1996) Zooplankton capture by two scleractinian corals, *Madracis mirabilis* and *Montastrea cavernosa*, in a field enclosure. Mar Biol 127:303–317
Storey KB, Storey JM (1990) Metabolic rate depression and biochemical adaptation in anaerobiosis, hibernation and estivation. Q Rev Biol 65:145–174
Thompson JR, Rivera HE, Closek CJ, Medina M (2015) Microbes in the coral holobiont: partners through evolution, development, and ecological interactions. Front Cell Infect Microbiol 4:176

Towle EK, Enochs IC, Langdon C (2015) Threatened Caribbean coral is able to mitigate the adverse effects of ocean acidification on calcification by increasing feeding rate. PLOS ONE 10:e0123394

Tremblay P, Grover R, Maguer JF, Legendre L, Ferrier-Pagès C (2012) Autotrophic carbon budget in coral tissue: a new ^{13}C-based model of photosynthate translocation. J Exp Biol 215:1384–1393

Tremblay P, Gori A, Maguer JF, Hoogenboom M, Ferrier-Pags C (2016) Heterotrophy promotes the re-establishment of photosynthate translocation in a symbiotic coral after heat stress. Sci Rep 6:38112

Van Woesik R, McCaffrey KR (2017) Repeated thermal stress, shading, and directional selection in the Florida reef tract. Front Mar Sci 4:182

Veal CJ, Holmes G, Nunez M, Hoegh-Guldberg O, Osborn J (2010) A comparative study of methods for surface area and three-dimensional shape measurement of coral skeletons. Limnol Oceanogr Methods 8:241–253

Wangpraseurt D, Larkum AWD, Ralph PJ, Kühl M (2012) Light gradients and optical microniches in coral tissues. Front Microbiol 3:316

Wangpraseurt D, Larkum AWD, Franklin J, Szabó M, Ralph PJ, Kühl M (2014) Lateral light transfer ensures efficient resource distribution in symbiont-bearing corals. J Exp Biol 217:489–498

Wangpraseurt D, Holm JB, Larkum AWD, Pernice M, Ralph PJ, Suggett DJ, Kühl M (2017) *In vivo* microscale measurements of light and photosynthesis during coral bleaching: evidence for the optical feedback loop? Front Microbiol 8:59

Wangpraseurt D, Jacques S, Lyndby NH, Holm JB, Ferrier-Pagès C, Kühl M (2019) Microscale light management and inherent optical properties of intact corals studied with optical coherence tomography. J R Soc Interface 16: 20180567

Weis VM (2008) Cellular mechanisms of Cnidarian bleaching: stress causes the collapse of symbiosis. J Exp Biol 211:3059–3066

Wellington GM (1982) An experimental analysis of the effects of light and zooplankton on coral zonation. Oecologia 52:311–320

Appendix.

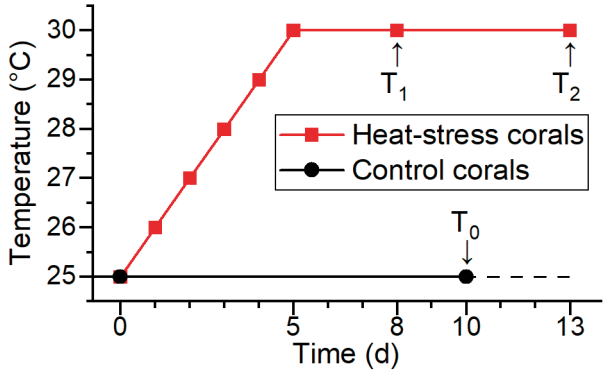

Fig. A1. Timeline of experiment. Corals were maintained in experimental tanks for 2 mo of acclimation at 25°C before onset of experiment. On Day 0, heat-stressed corals were subjected to thermal stress by ramping aquarium temperature (1°C d^{-1}), until a temperature of 30°C was reached. T_0, T_1 and T_2 indicate when measurements were performed on respective corals

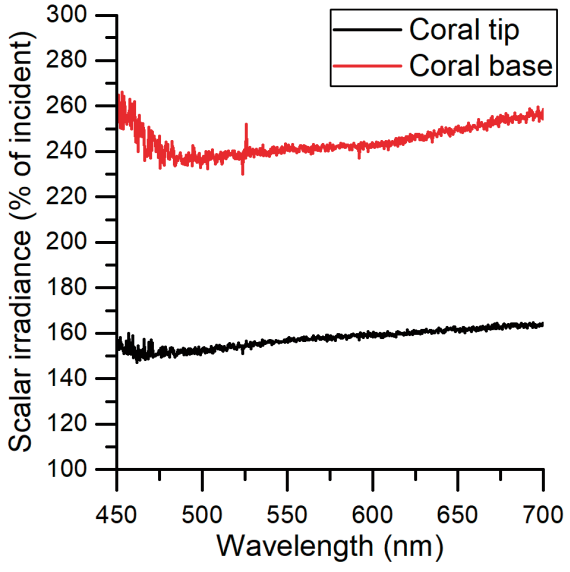

Fig. A2. Surface scalar irradiance measurements on bare *Pocillopora damicornis* skeletons. Red plot represents measurements near the base of the coral branch and black at the very tip of the apical branch. Scalar irradiance spectra are normalized to the incident photon irradiance. Data are mean (n = 3). See Lyndby et al. (2019) for further details on data acquisition

Editorial responsibility: Joseph Pawlik, Wilmington, North Carolina, USA

Submitted: May 11, 2020; Accepted: August 18, 2020
Proofs received from author(s): October 9, 2020